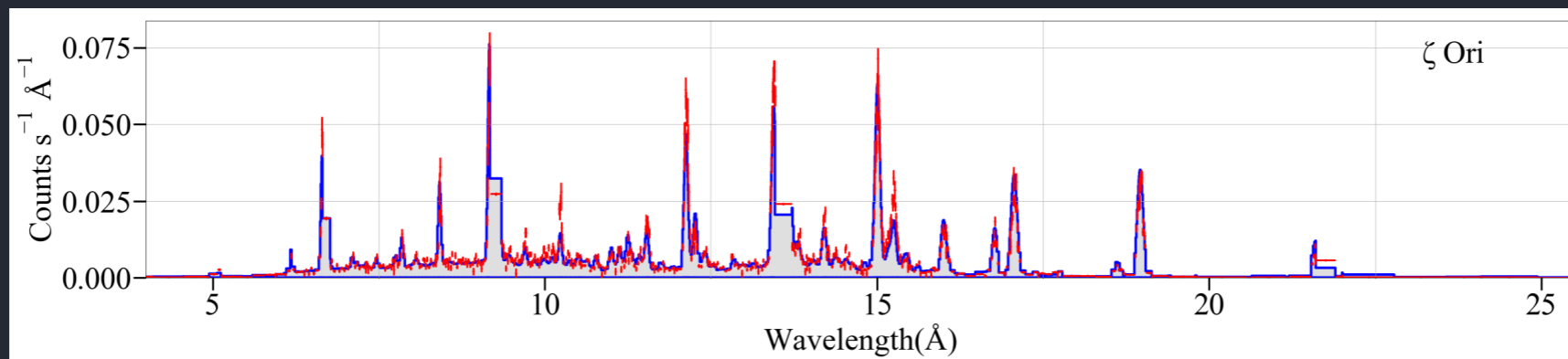
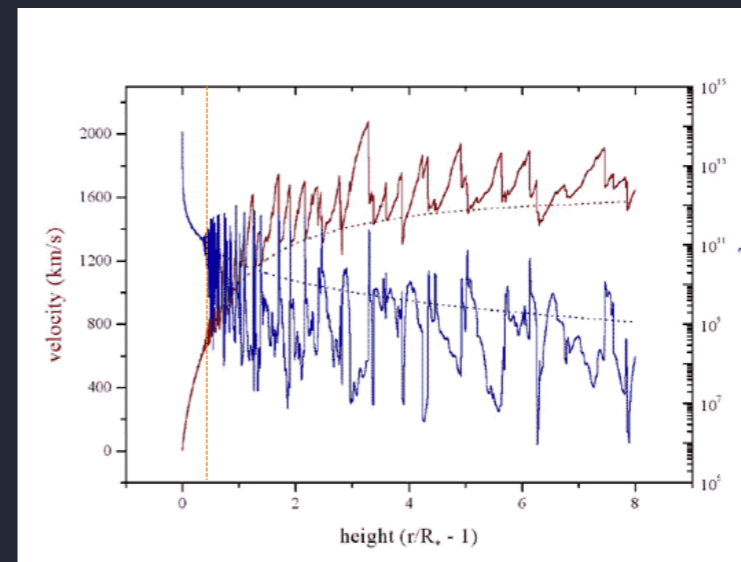


# O Star Winds: Shocked Plasma Temperatures and Mass-Loss Rates

Vaughn Parts  
Swarthmore College

David Cohen (Swarthmore College), Véronique Petit and Stan Owocki (University of Delaware), Jon Sundqvist (Leuven University), Maurice Leutenegger (Goddard Spaceflight Center), Marc Gagné (West Chester University)

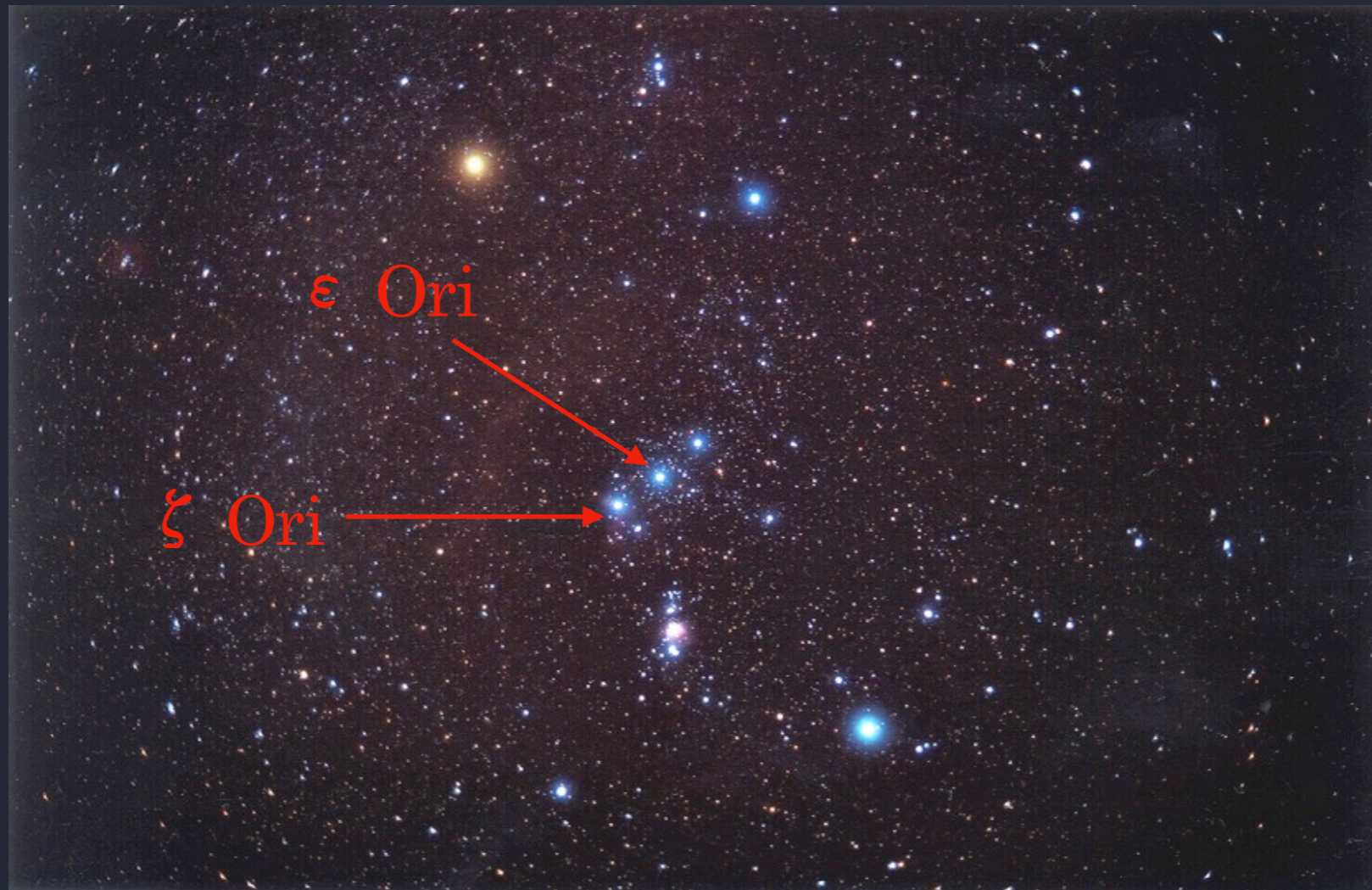


# Our Sample

Effectively single, non-magnetic

Typical mass-loss rate  $\sim 10^{-6} M_{\text{sun}} \text{ yr}^{-1}$

Wind terminal velocity  $\sim 2,000 \text{ km s}^{-1}$



# Our Sample



Effectively single, non-magnetic

Typical mass-loss rate  $\sim 10^{-6} M_{\text{sun}} \text{ yr}^{-1}$

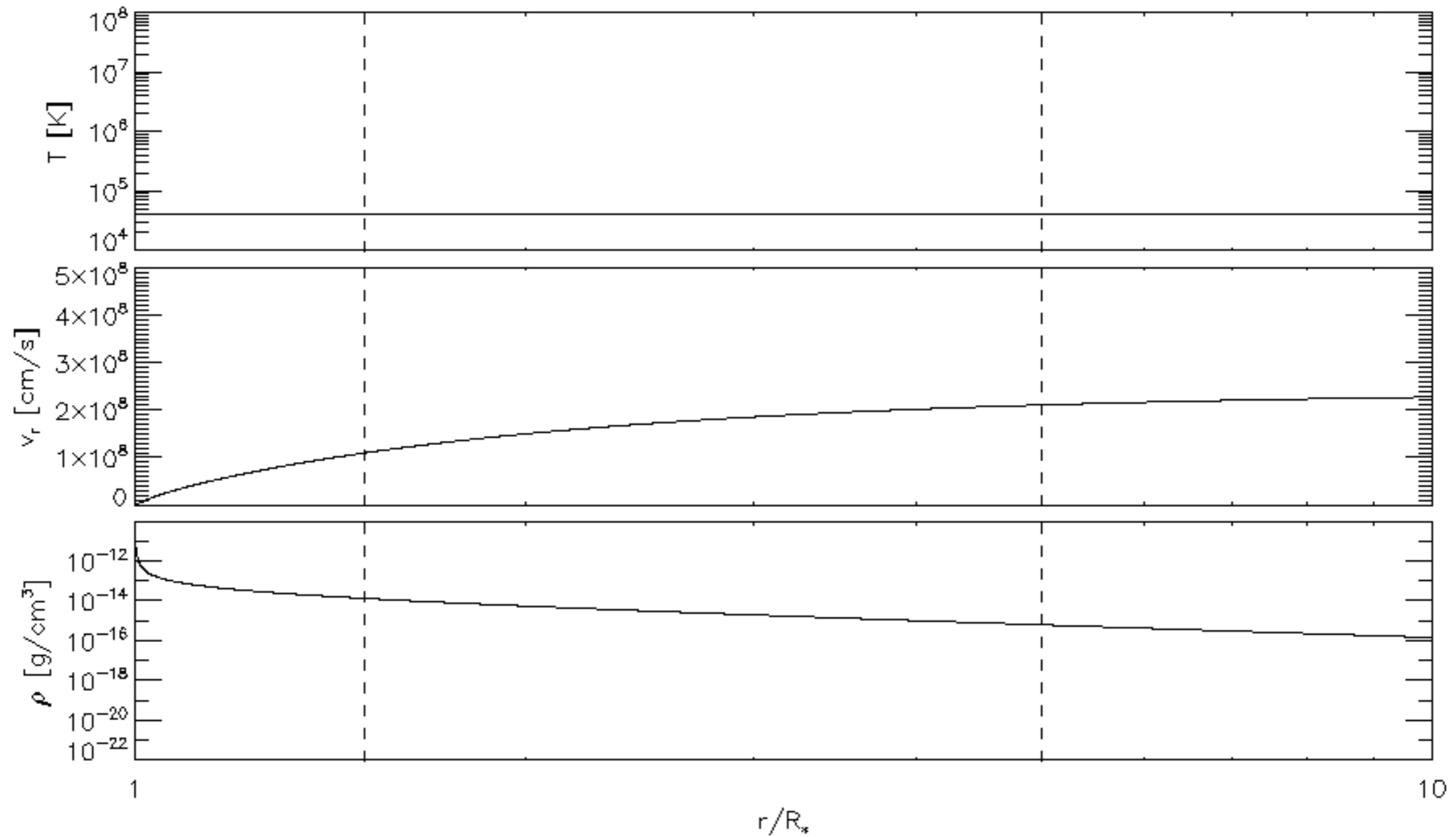
Wind terminal velocity  $\sim 2,000 \text{ km s}^{-1}$

Star	Spectral Type	Distance (pc)	$R_*$ ( $R_{\odot}$ )	$v_{\infty}$ ( $\text{km s}^{-1}$ )	$\dot{M}_{\text{theory}}$ ( $M_{\odot} \text{ yr}^{-1}$ )	$N_{\text{ISM}}$ ( $10^{22} \text{ cm}^{-2}$ )
$\zeta$ Pup	O4 If	460 <sup>c</sup>	18.9 <sup>d</sup>	2250	$6.4 \times 10^{-6}$	0.01
9 Sgr	O4 V	1300 <sup>a</sup>	12.4 <sup>b</sup>	3100	$2.1 \times 10^{-6}$	0.22
$\zeta$ Ori	O9.7 Ib	226 <sup>e</sup>	22.1 <sup>b</sup>	1850	$1.2 \times 10^{-6}$	0.03
$\epsilon$ Ori	B0 Ia	363 <sup>g</sup>	32.9 <sup>g</sup>	1600	$1.2 \times 10^{-6}$	0.03
$\xi$ Per	O7.5 III	382 <sup>e</sup>	14.0 <sup>f</sup>	2450	$9.3 \times 10^{-7}$	0.11
$\zeta$ Oph	O9.5 V	112 <sup>e</sup>	8.9 <sup>f</sup>	1550	$1.8 \times 10^{-7}$	0.06

# X-Rays from Embedded Wind Shocks (EWS)

- Line Deshadowing Instability (LDI) leads to shock-heating of wind
- heated plasma cools by radiating x-rays
- many shocks above  $\sim 1.5R_{\text{star}}$

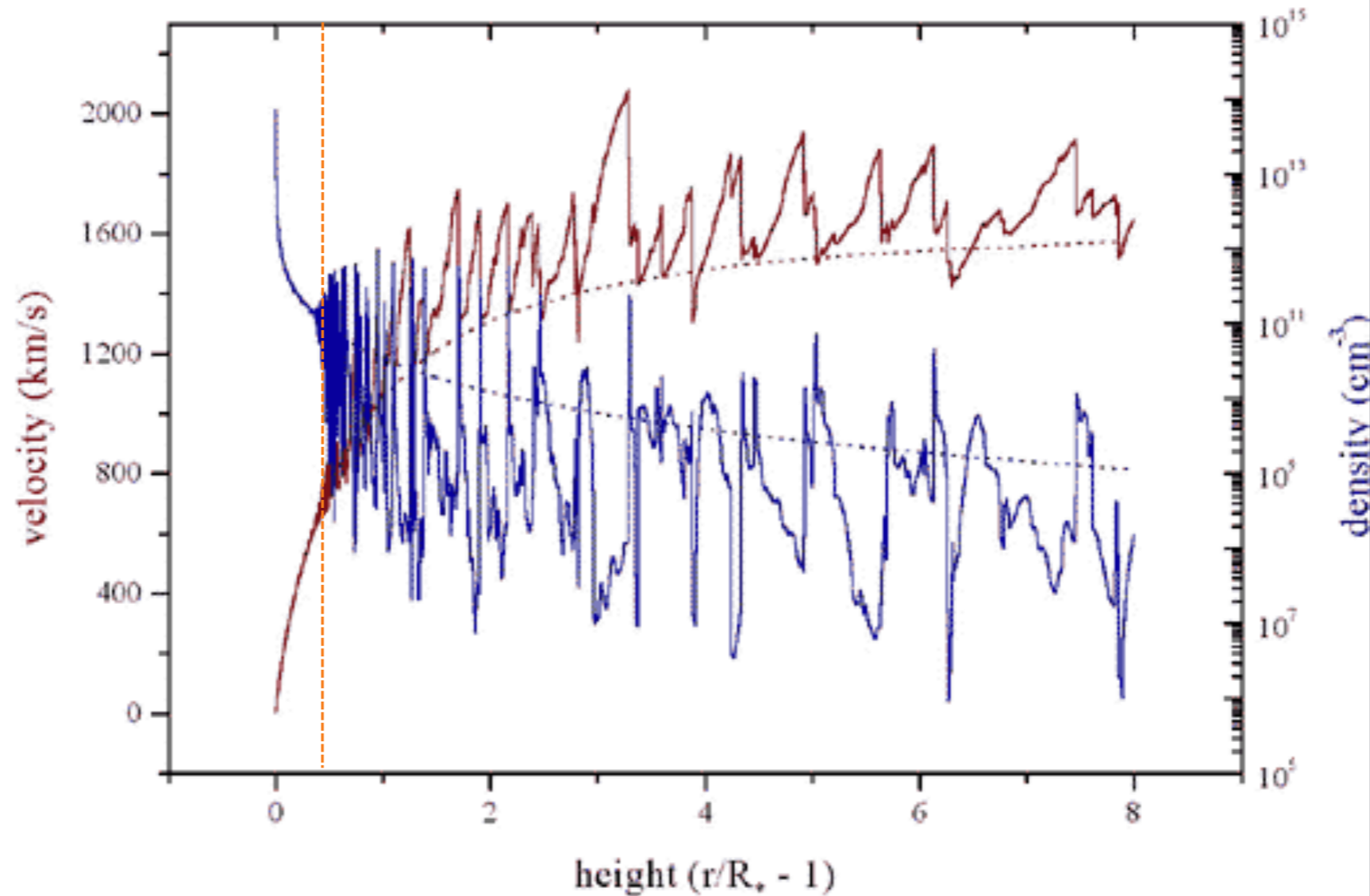
1-D hydro simulation (J. Sundqvist)



# Shocked Wind Structure

- reverse shocks dominate: pre-shock velocity  $>$  ambient wind velocity
- post-shock  $T \sim$  few  $10^6$  K up to few  $10^7$  K
- but 99% of wind is cold, **absorbs** x-rays

1-D hydro simulation (J. Sundqvist)

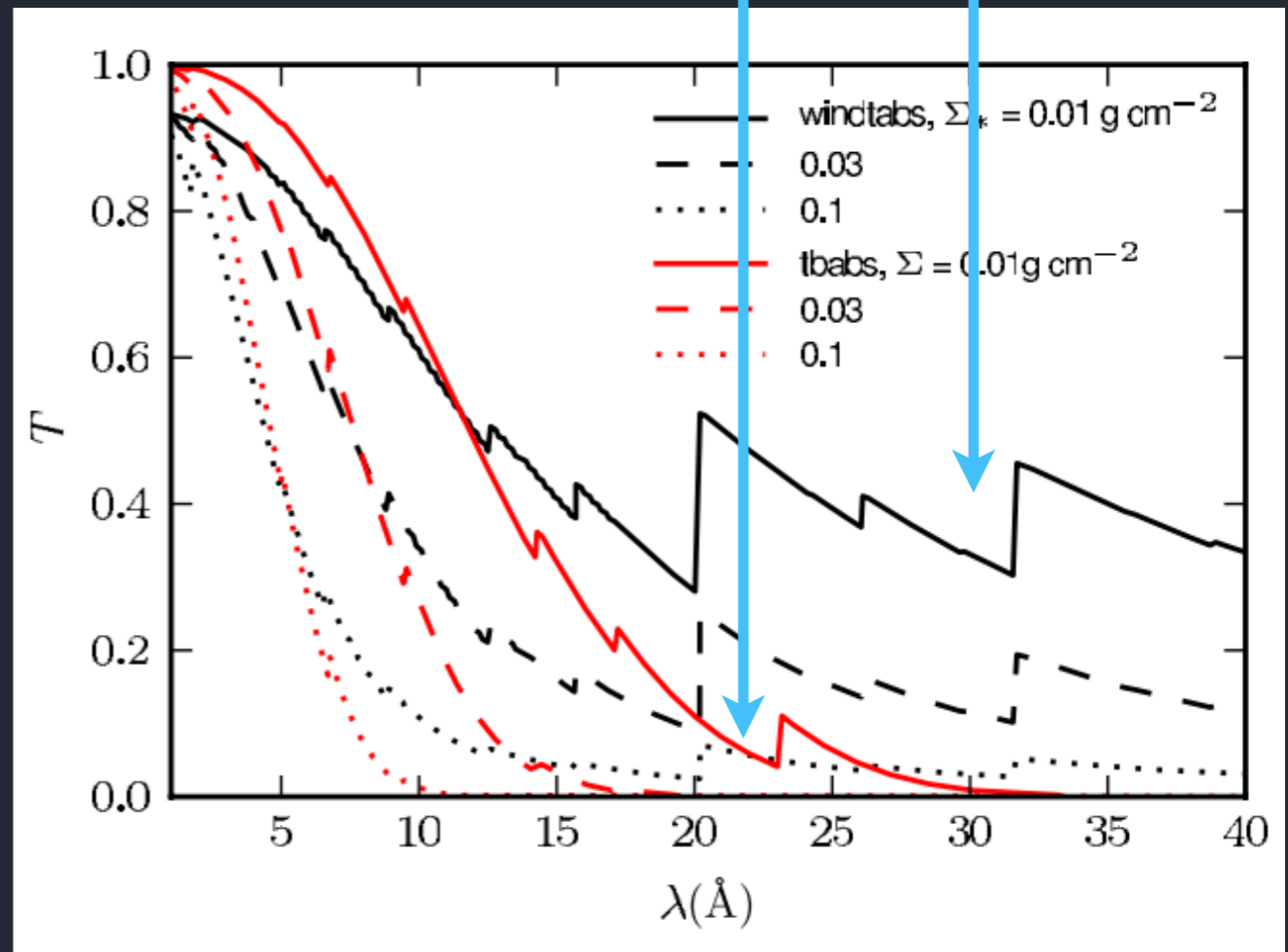
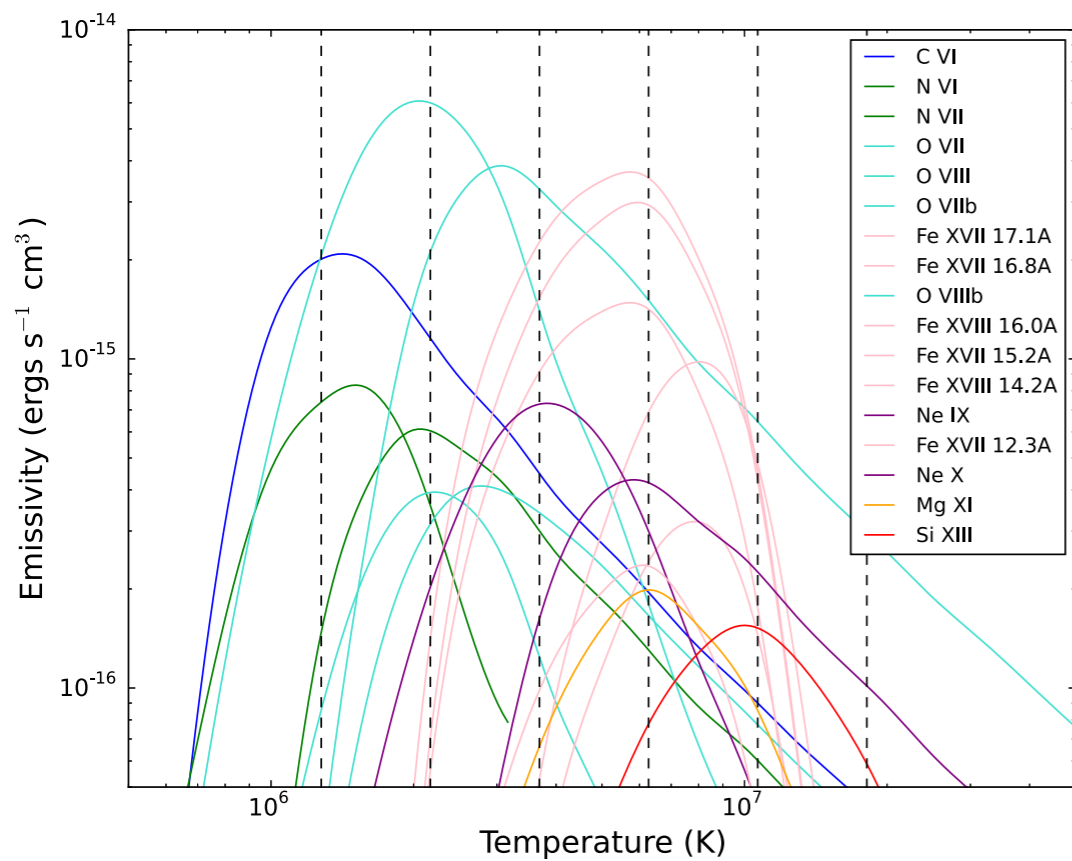


# Our Model

- 6 fixed-temperature **bvapec** emission components
- $\log(T)$  spacing samples lines' peak emissivities
- **windtabs** wind absorption: spatially distributed
- **tbabs** ISM absorption

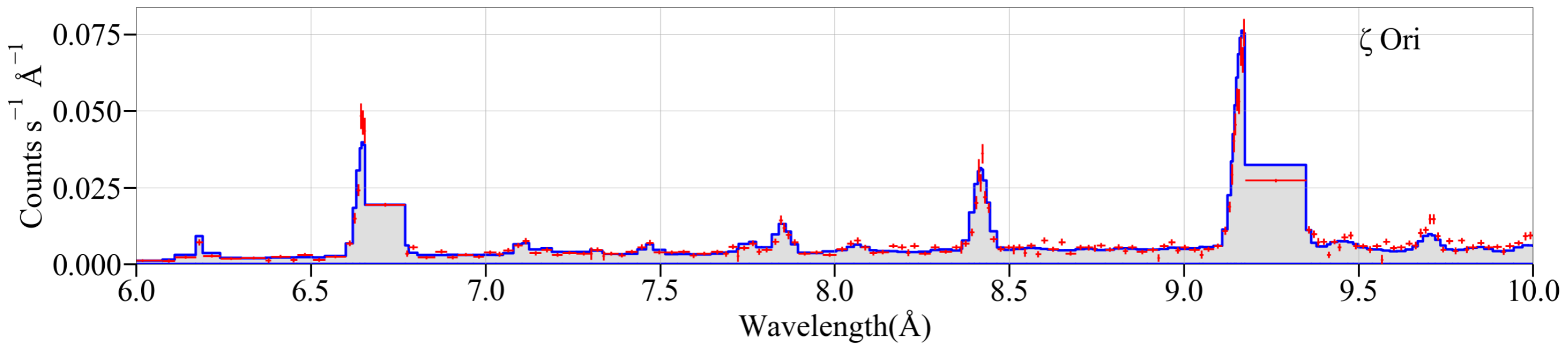
windtabs

slab



# Fitting

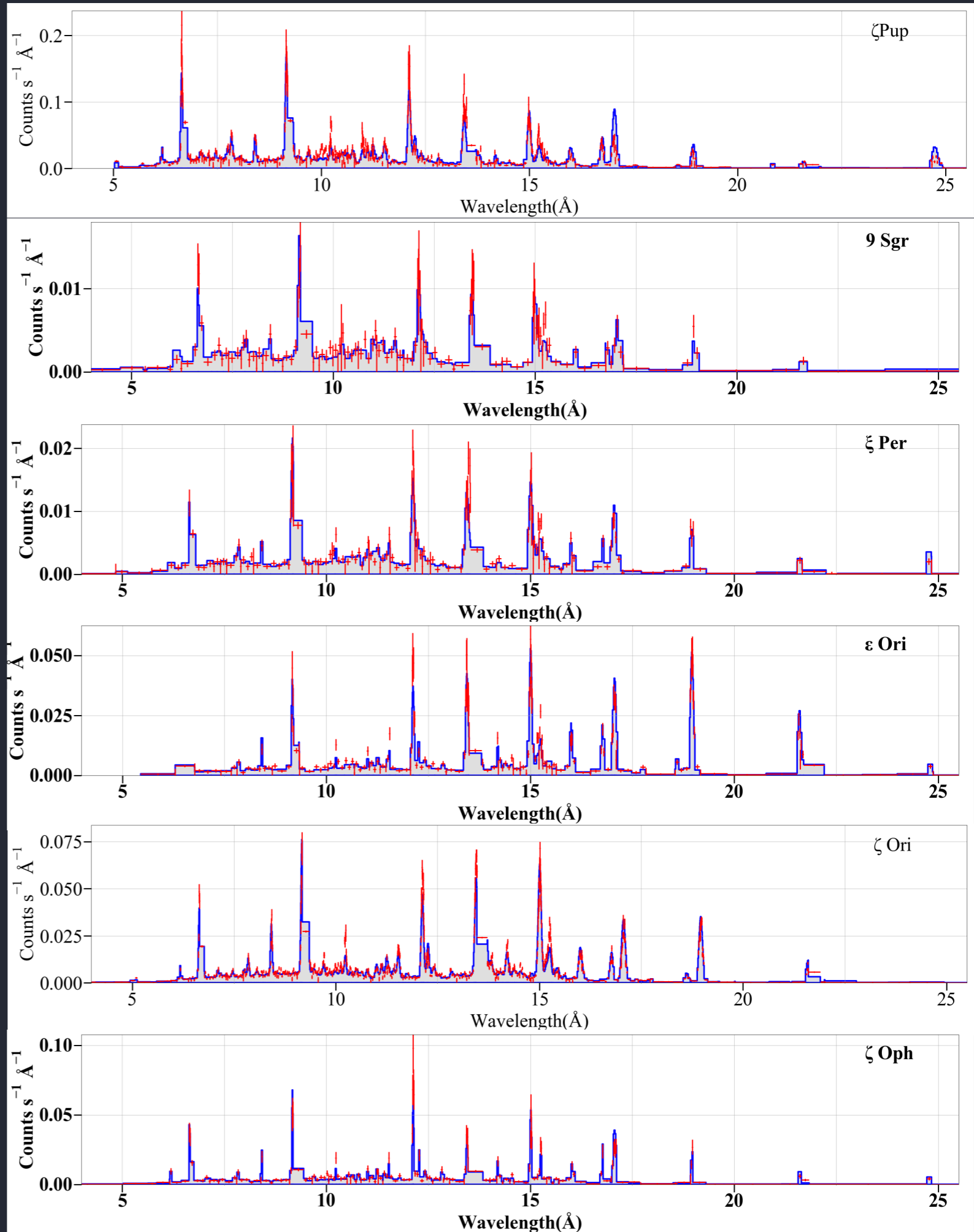
- lines and continuum fit well
- data are adaptively grouped and f,i lines grouped



# Fitting (continued)

- a consistent method for our 6 stars fits all stars well
- DEMs and mass-loss rates determined
- line widths consistent w/ wind terminal velocities
- N elevated in stars like  $\zeta$  Pup, where expected

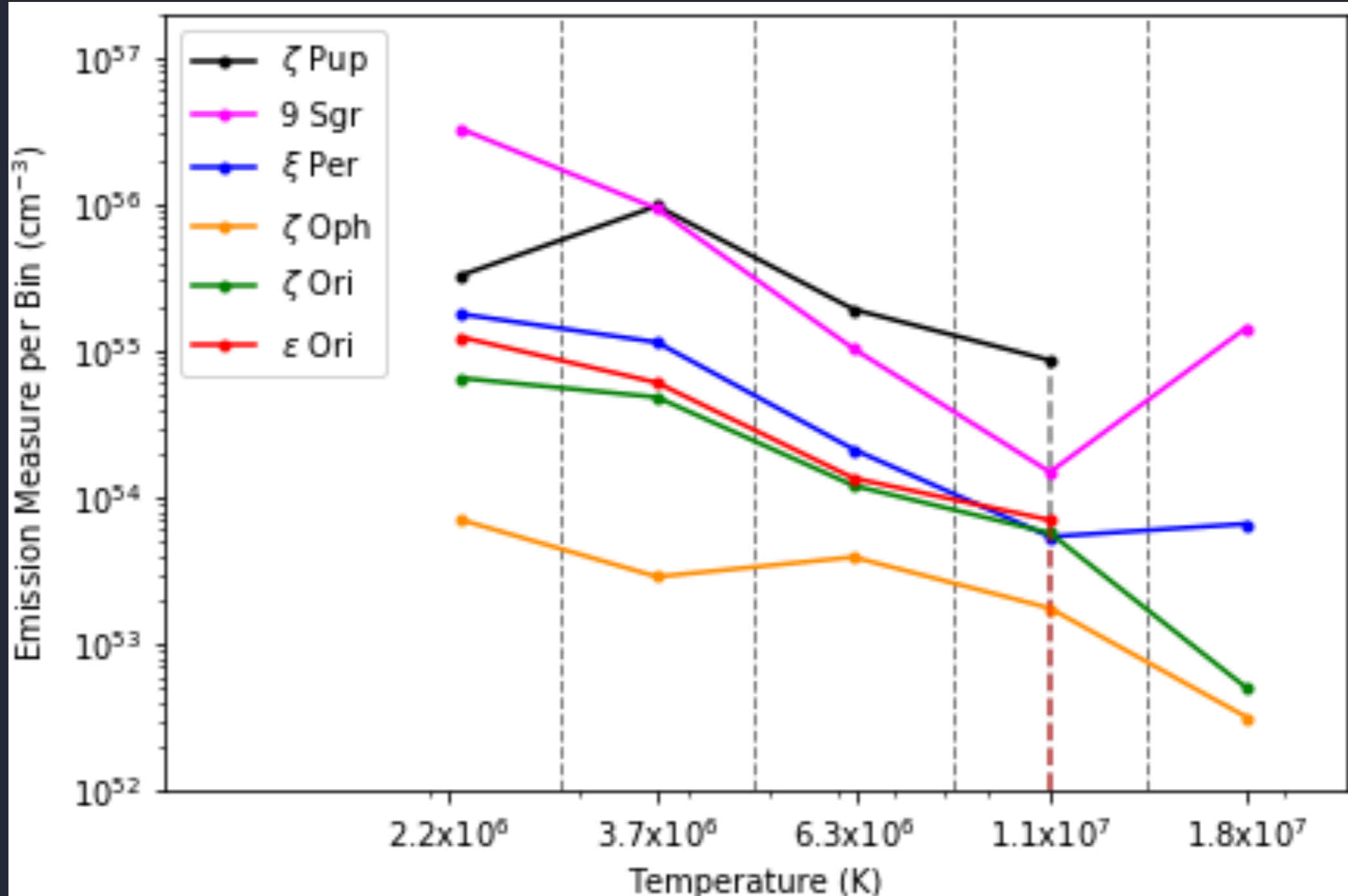
This model fitting technique is a compromise between detailed non-LTE multi wavelength wind modeling and simple variable-two-temperature and excess-ISM absorption modeling





# EM vs. T

- universal shape (power law w/ slope  $\sim -2.5$ )
- very little emission above  $12 \times 10^6$  K ( $<2\%$  of total)
- broadly consistent with LDI

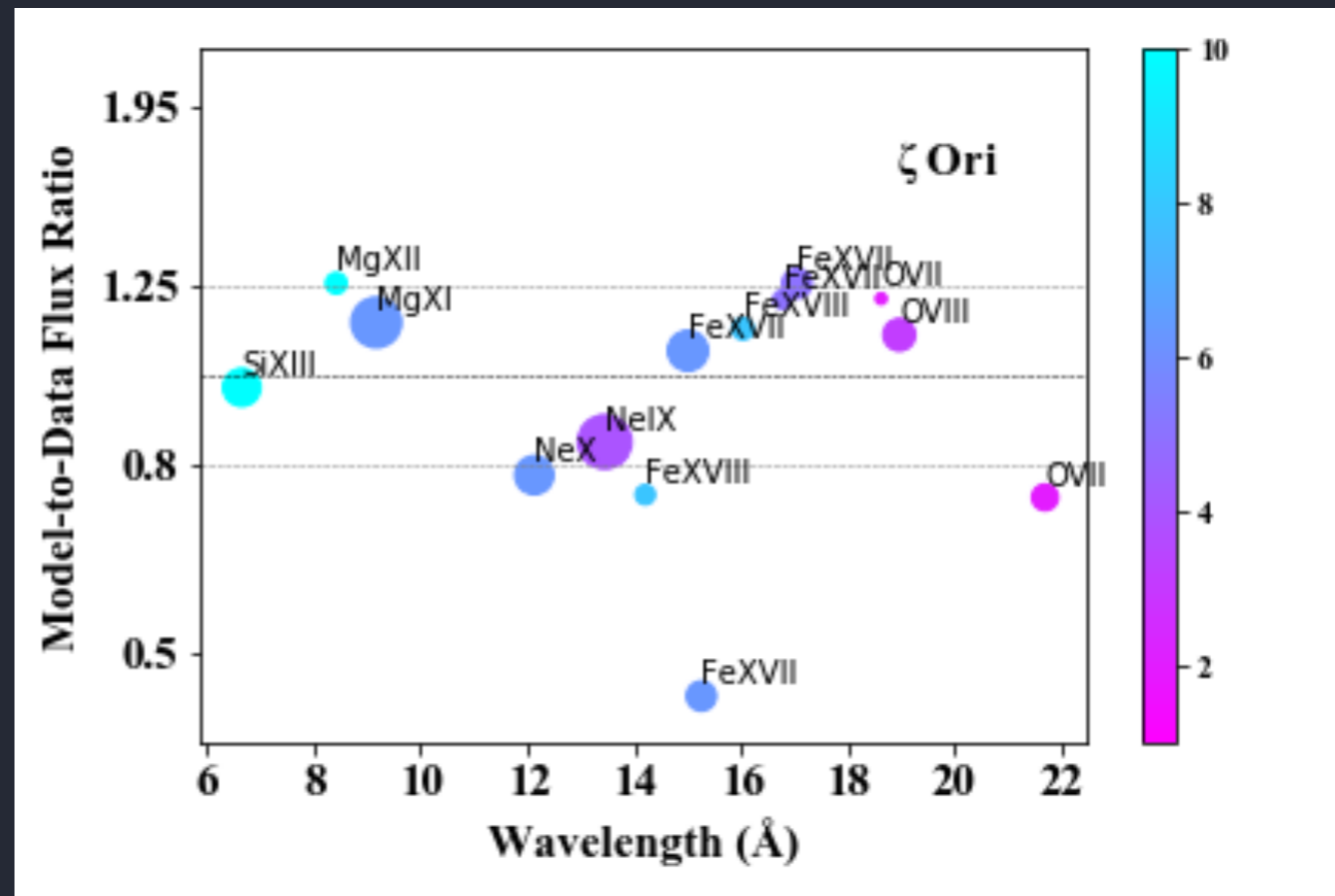
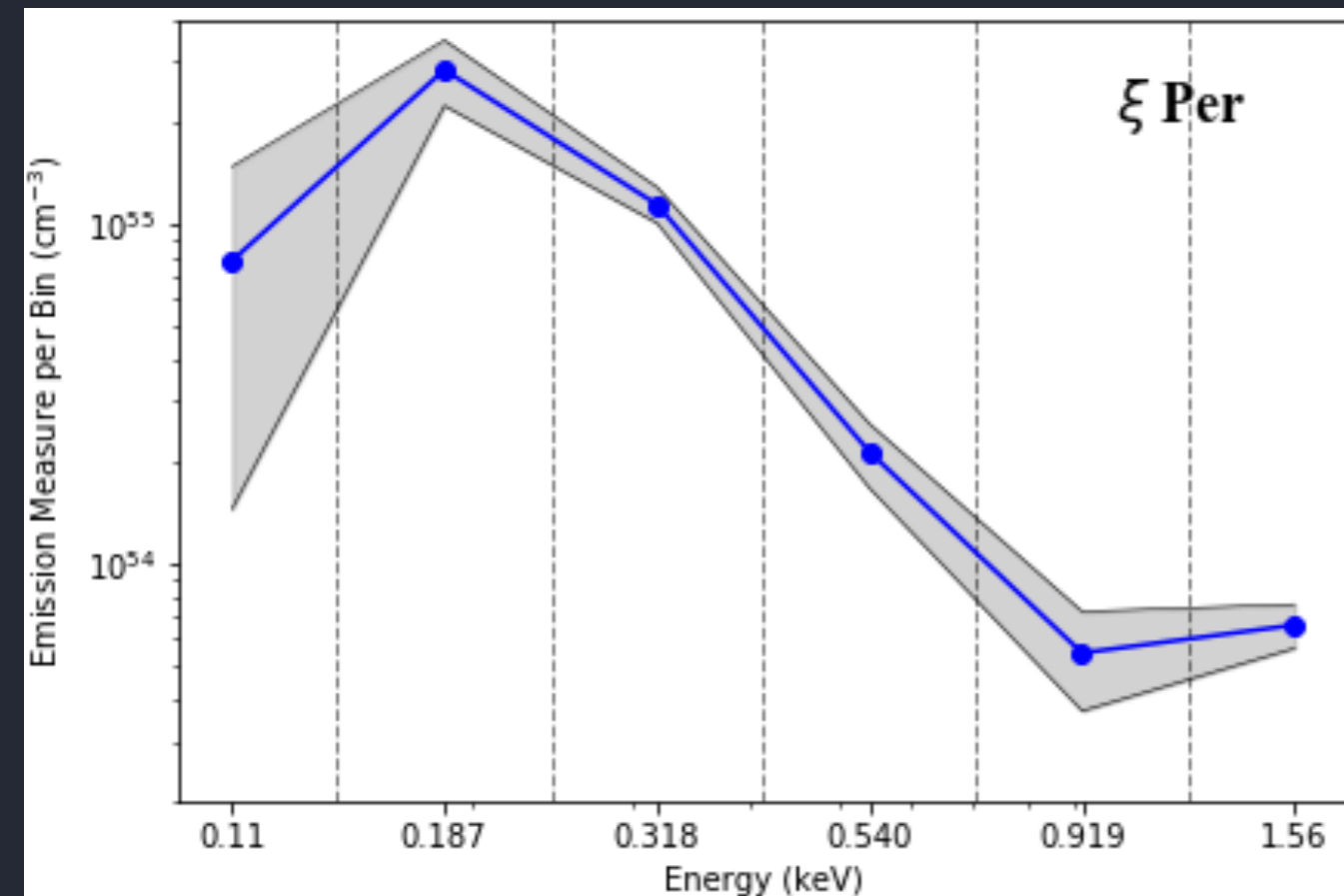


formally good fits

EM vs. T well constrained

statistically poor fits

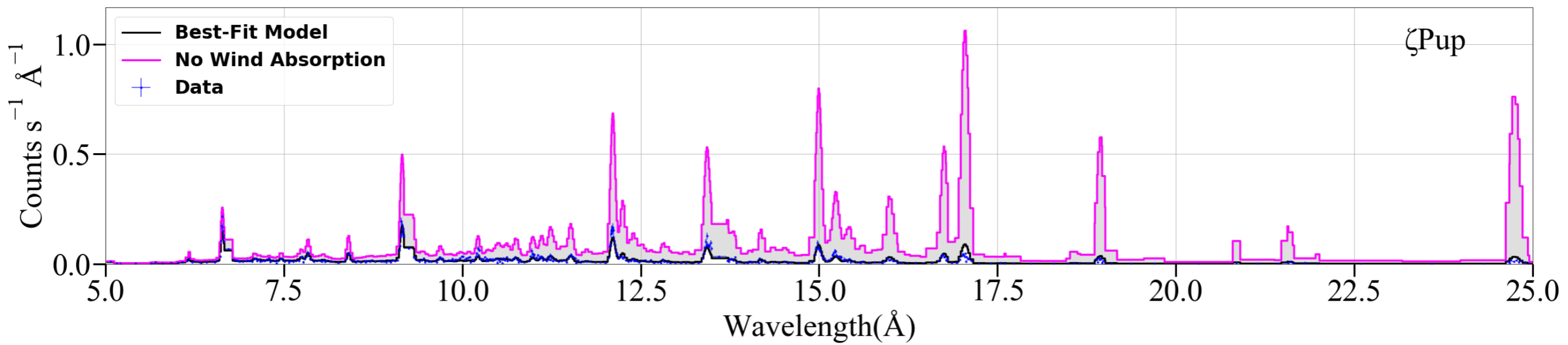
line flux ratios agree within 25%



- high S/N data, dominated by systematics
- atomic physics model uncertainties, line shapes

# Wind Absorption

- $\sim 90\%$  of emitted X-ray flux from  $\zeta$  Pup is absorbed by the wind
- the wind absorption provides a mass-loss rate measurement



# Mass-Loss Rates

Star	Spectral Type	Theory: Vink et al. 2001 ( $M_{\odot} \text{ yr}^{-1}$ )	Cohen et al. 2014 ( $M_{\odot} \text{ yr}^{-1}$ )	this work ( $M_{\odot} \text{ yr}^{-1}$ )
$\zeta$ Pup	O4 I	$6.4 \times 10^{-6}$	$1.8 \times 10^{-6}$	$1.5 \times 10^{-6}$
9 Sgr	O4 V	$2.1 \times 10^{-6}$	$3.7 \times 10^{-7}$	$5.4 \times 10^{-7}$
$\zeta$ Ori	O9.7 I	$1.2 \times 10^{-6}$	$3.4 \times 10^{-7}$	$3.9 \times 10^{-7}$
$\epsilon$ Ori	B0 I	$1.2 \times 10^{-6}$	$6.5 \times 10^{-7}$	$4.3 \times 10^{-7}$
$\xi$ Per	O7.5 III	$9.3 \times 10^{-7}$	$2.2 \times 10^{-7}$	$5.1 \times 10^{-7}$
$\zeta$ Oph	O9 V	$1.8 \times 10^{-7}$	$1.5 \times 10^{-9}$	$1.2 \times 10^{-7}$

- consistent with determinations from other methods: X-ray line profiles, H-alpha and radio free-free that includes clumping
- lower than classic Vink et al. (2001) theoretical calculations



# Extra Slides

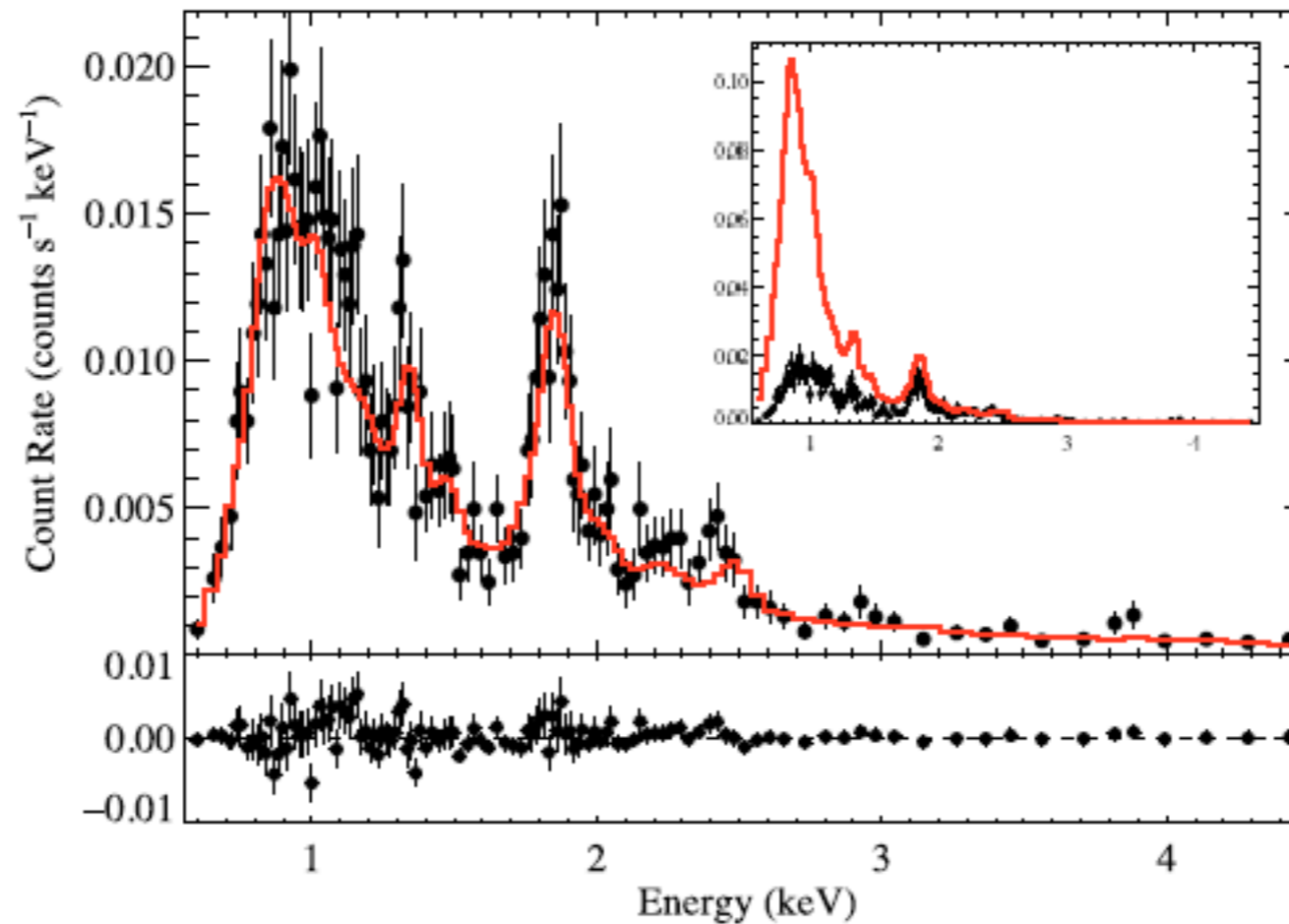


**Figure 9.** The same zeroth order ACIS CCD spectrum shown in Fig. 2, here fit with a two-temperature *apec* thermal emission model (red histogram), where one temperature component (0.6 keV) is attenuated by the stellar wind as well as the interstellar medium and the other (3.3 keV) is attenuated only by the ISM. Note the presence of strong Si XIII emission just below 2 keV. The vast majority of the emission in this spectrum is line emission, but due to the low resolution of the detector as well as the presence of many weak, blended lines, the spectrum looks relatively smooth. The inset figure shows the same data with a model identical to the best-fit model, except that the wind absorption ( $\Sigma_*$  in *windtabs*) is zeroed out. This model spectrum makes the significance of the wind absorption effect quite obvious. Nearly 80% of the emitted EWS X-rays are absorbed before they can escape from the wind.

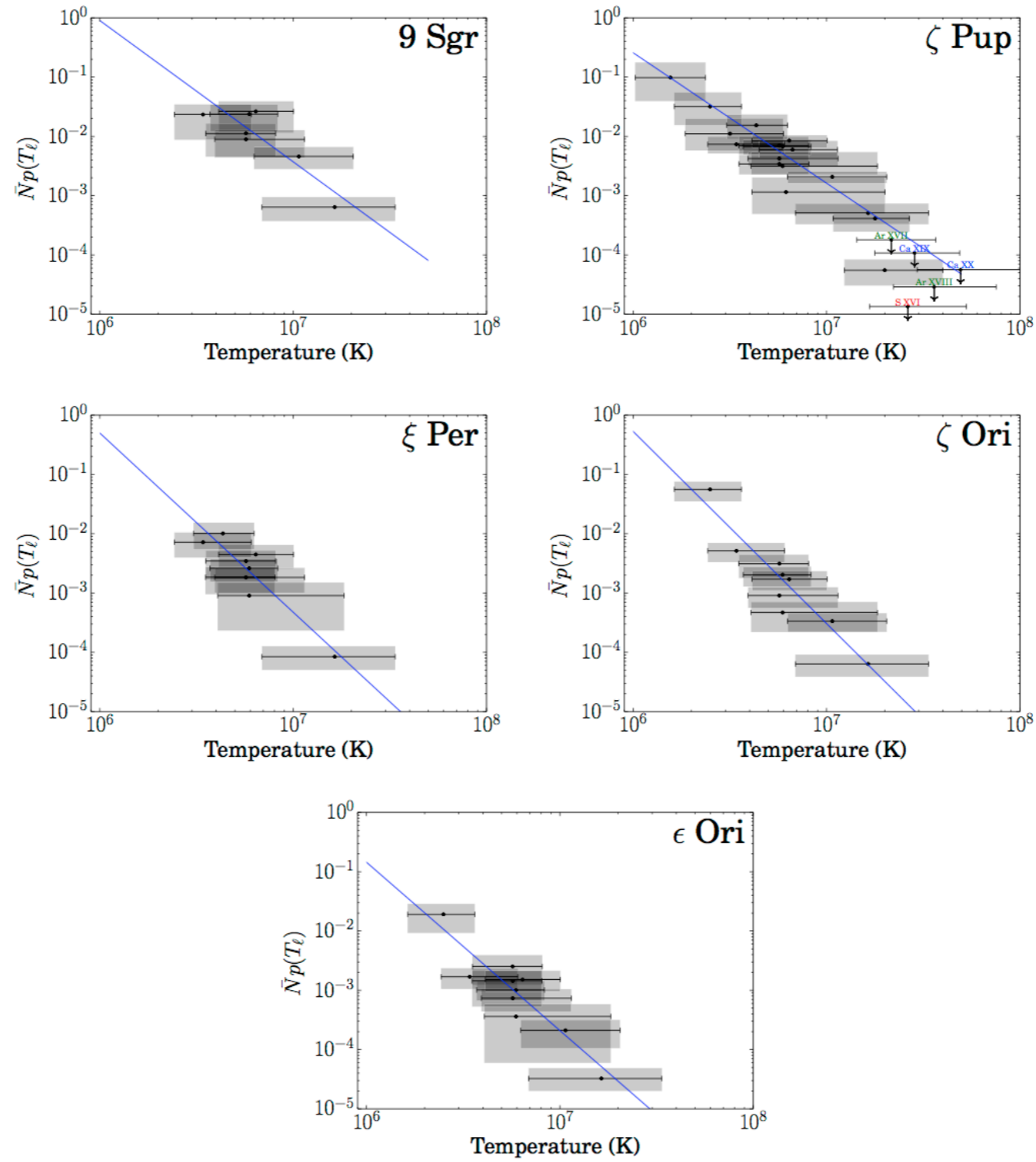


**Figure 5.** The shock heating rate,  $\bar{N}p(T_l)$ , is shown with the uncertainty on its value (vertical extent of each gray box) as well as the FWHM of the line emissivity ratio,  $\Lambda_l(T)/\Lambda(T)$  (horizontal extent, visually reinforced by the horizontal error bars). The points are at  $T_l$  for each line. The best-fit power law to each set of values is shown as a blue line in each panel. For  $\zeta$  Pup, the lowest temperature point corresponds to the N VI feature measured with *XMM-Newton*. And for this star, upper limits are included for five additional lines, none of which are detected in the *Chandra* spectrum.



Chandra MEG  $m = \pm 1$

4 T apec + *windtabs* + ISM

4 T apec + slab + ISM

